ОБЪЕДИНЕННЫЙ
ИНСТИТУТ
ЯДЕРНЫХ
ИССЛЕДОВАНИЙ

Дубна

E2-99-5

G.N.Afanasiev[1], V.G.Kartavenko, Yu.P.Stepanovsky[2]

ON TAMM'S PROBLEM IN THE VAVILOV–CERENKOV RADIATION THEORY

Submitted to «Journal of Physics D: Applied Physics»

[1]E-mail: afanasiev@thsun1.jinr.ru
[2]The Institute of Physics and Technology, Kharkov, Ukraine

1999

Афанасьев Г.Н., Картавенко В.Г., Степановский Ю.П. E2-99-5
О задаче Тамма в теории излучения Вавилова–Черенкова

Дан анализ известной задачи Тамма, которая описывает движение заряженной частицы на конечном интервале со скоростью, превышающей скорость света в веществе. Из сравнения приближенных формул Тамма с точными следует, что формулы Тамма не описывают адекватно черенковское излучение. Также проанализирована известная формула Тамма $\cos\theta_T = 1/\beta n$, определяющая максимум Фурье-компонент напряженностей поля. Численный анализ показывает, что Фурье-компоненты напряженностей поля имеют четко выраженный максимум при $\theta = \theta_T$ только для достаточно малого интервала движения заряженной частицы. С увеличением интервала движения появляется много максимумов. Для движения на бесконечном интервале напряженности поля состоят из бесконечного числа максимумов одинаковой амплитуды. Квантовый анализ формулы Тамма приводит к тем же результатам.

Работа выполнена в Лаборатории теоретической физики им. Н.Н.Боголюбова ОИЯИ.

Препринт Объединенного института ядерных исследований. Дубна, 1999

Afanasiev G.N., Kartavenko V.G., Stepanovsky Yu.P. E2-99-5
On Tamm's Problem in the Vavilov–Cerenkov Radiation Theory

We analyse the well-known Tamm's problem treating the charge motion on a finite space interval with the velocity exceeding light velocity in medium. By comparing Tamm's approximate formulae with the exact ones we prove that the former do not properly describe Cerenkov radiation terms. We also investigate Tamm's formula $\cos\theta_T = 1/\beta n$ defining the position of the maximum of the field strengths in the Fourier representation. Numerical analysis of the Fourier components of field strengths shows that they have a well pronounced maximum at $\theta = \theta_T$ only for the charge motion on the sufficiently small interval. As an interval grows, many maxima appear. For the charge motion on an infinite interval there is infinite number of maxima of the same amplitude. The quantum analysis of Tamm's formula leads to the same results.

The investigation has been performed at the Bogoliubov Laboratory of Theoretical Physics, JINR.

Preprint of the Joint Institute for Nuclear Research. Dubna, 1999

1 Introduction

In 1888 O. Heaviside considered an infinite charge motion in the nondispersive dielectric infinite medium [1]. He showed that a specific radiation arises when the charge velocity v exceeds the light velocity in medium c_n. This radiation is confined to the cone with a solution angle $\sin\theta_c = 1/\beta_n$. Here $\beta_n = v/c_n$. The Poynting vector being perpendicular to this cone has the angle

$$\cos\theta_c = 1/\beta_n \tag{1.1}$$

with the motion axis. This radiation was experimentally observed by P.A. Čerenkov in 1934 [2]. Unfortunately, Heaviside's studies had been forgotten until 1974 when they were revived by A.A. Tyapkin [3] and T.R. Kaiser [4].

I.E. Tamm and I.M. Frank [5] without knowing the previous Heaviside investigations explained Čerenkov's experiments solving the Maxwell equations in the Fourier representation and subsequently returning to the usual space-time representation. The use of the Fourier representation permitted them to treat the dispersive media as well. For the non-dispersive media they confirmed the validity of Eq.(1.1) defining the direction of the Čerenkov radiation.

In 1939 I.E.Tamm [6] considered the uniform motion of a point charge on the finite space interval with the velocity v exceeding the light velocity in medium c_n. Here $c_n = c/n(\omega)$, $n(\omega)$ is the frequency-dependent refraction index of the medium. He showed that Fourier components of electromagnetic field strengths have a sharp maximum at the angle

$$\cos\theta_T = 1/\beta_n \tag{1.2}$$

with the motion axis. Here $\beta_n = v/c_n(\omega)$. Later (see, e.g., [7]) Eq.(1.2) was applied to the charge motion in an infinite medium.

On the other hand, in Ref. [8] the uniform motion of a point charge was considered in an infinite dispersive medium with a one-pole electric permittivity $\epsilon = n^2$ chosen in a standard way [9]:

$$\epsilon(\omega) = 1 + \frac{\omega_L^2}{\omega_0^2 - \omega^2}. \tag{1.3}$$

This expression is a suitable extrapolation between the static case $\epsilon(0) = 1 + \omega_L^2/\omega_0^2$ and the high-frequency limit $\epsilon(\infty) = 1$. The electromagnetic potentials, field strengths and the energy flux were evaluated on the surface of a cylinder co-axial with the charge axis motion z. They had the main maximum at those points of the cylinder surface where in the absence of dispersion it intersects by the Čerenkov singular cone and smaller maxima in the interior of this cone. On the other hand, the Fourier transforms of these quantities were oscillating functions of z and, therefore, of the scattering angle θ ($z = r\cos\theta$) without a pronounced maximum at $\cos\theta = 1/\beta_n$. This disagrees with the validity of Eq.(1.2) (not (1.1)) for the infinite charge motion.

Further, Zrelov and Ruzicka ([10,11]) numerically investigated Tamm's problem and came to the paradoxical result that Tamm's formulae (which, as they believed, describe Čerenkov's radiation) can be interpreted as interference of two bremsstrahlung (BS) waves emitted at the beginning and end of motion.

Slightly later the exact solution of the same problem in the absence of dispersion has been found in [12]. It was shown there that Čerenkov's radiation can by no means be

reduced to the interference of two BS waves.
These inconsistencies and the fact that formula (1.2) is widely used for the identification of Čerenkov radiation even for the uniform infinite charge motion enable us to reexamine Tamm's problem anew.

The plan of our exposition is as follows. In Sect. 2, we reproduce step by step the derivation of Tamm's formulae. In Sect. 3, by comparing approximate Tamm's formulae with exact ones we prove that they do not describe Čerenkov's radiation properly. The reason for this is due to the approximations involved in their derivation. Quantum analysis of Tamm's formula is given in Sect. 4. In Sect. 5, we analyze the validity of Tamm's formula (1.2) for different intervals of charge motion. We conclude that it is certainly valid for small intervals and breaks for larger ones. This is also supported by the analytical formula available for the infinite charge motion. On the other hand, the Tamm-Frank formula (1.1) is valid even for the dispersive media: it approximately defines the position of main intensity maximum in the usual space-time representation ([8]). A short discussion of the results obtained is given in section 6.

Some precaution is needed. When experimentally investigating charge motion on a finite interval [13], one usually considers an electron beam entering a thin transparent slab from vacuum , its propagation inside the slab and the subsequent passing into the vacuum on the other side of the slab. The so-called transition radiation ([14]) arises on the slab interfaces. In this investigation we deal with a pure Tamm's problem: electron starts at a given point in medium, propagates with a given velocity and then stops at a second point. This may be realized, e.g., for the electron propagation in water where the distance between successive scatters is $\approx 1\mu m$, which is approximately twice the wavelength of the visible Čerenkov radiation [15].

2 Tamm's problem

Tamm considered the following problem. The point charge rests at the point $z = -z_0$ of the z axis up to a moment $t = -t_0$. In the time interval $-t_0 < t < t_0$ it uniformly moves along the z axis with the velocity v greater than the light velocity in medium c_n. For $t > t_0$ the charge again rests at the point $z = z_0$. The non-vanishing z Fourier component of the vector potential (VP) is given by

$$A_\omega = \frac{1}{c}\int_{-z_0}^{z_0}\frac{1}{R}j_\omega(x',y',z')\exp\left(-i\omega R/c\right)dx'dy'dz',$$

where $R = [(x-x')^2 + (y-y')^2 + (z-z')^2]^{1/2}$, $j_\omega = 0$ for $z' < -z_0$ and $z' > z_0$ and $j_\omega = e\delta(x')\delta(y')\exp(-i\omega z'/v)/2\pi$ for $-z_0 < z' < z_0$. Inserting all this into A_ω and integrating over x' and y' one gets

$$A_\omega(x,y,z) = \frac{e}{2\pi c}\int_{-z_0}^{z_0}\frac{dz'}{R}\exp\left[-i\omega\left(\frac{z'}{v}+\frac{R}{c_n}\right)\right],$$
$$R = [\rho^2 + (z-z')^2]^{1/2}, \quad \rho^2 = x^2 + y^2. \tag{2.1}$$

At large distances from the charge ($R >> z_0$) one has : $R = R_0 - z'\cos\theta$, $\cos\theta = z/R_0$. Inserting this into (2.1) and integrating over z' one gets

$$A_\omega(\rho,z) = \frac{e\beta q(\omega)}{\pi R_0\omega}\exp\left(-i\omega R_0/c_n\right), \quad q(\omega) = \frac{\sin\left[\omega t_0(1-\beta_n\cos\theta)\right]}{1-\beta_n\cos\theta}. \tag{2.2}$$

Now we evaluate the field strengths. In the wave zone where $R_0 >> c/n\omega$ one obtains

$$H_\phi = -\frac{2e\beta}{\pi c R_0}\sin\theta\int_0^\infty nq(\omega)\sin[\omega(t-R_0/c_n)]d\omega,$$

$$E_\rho = -\frac{2e\beta}{\pi c R_0}\sin\theta\cos\theta\int_0^\infty q(\omega)\sin[\omega(t-R_0/c_n)]d\omega,$$

$$E_z = \frac{2e\beta}{\pi c R_0}\sin^2\theta\int_0^\infty q(\omega)\sin[\omega(t-R_0/c_n)]d\omega. \qquad (2.3)$$

It should be noted that only the θ spherical component of $\vec{E}$ differs from zero

$$E_r = 0, \quad E_\theta = -\frac{2e\beta}{\pi c R_0}\sin\theta\int_0^\infty q(\omega)\sin[\omega(t-R_0/c_n)]d\omega.$$

Consider now the function $q(\omega)$. For $\omega t_0 >> 1$ it goes into $\pi\delta(1-\beta_n\cos\theta)$. This means that under these conditions $\vec{E}_\omega$ and $\vec{H}_\omega$ have a sharp maximum for $1-\beta_n\cos\theta = 0$. Or, in other words, photons with the energy $\hbar\omega$ should be observed at the angle $\cos\theta = 1/\beta_n$.

The energy flux through the sphere of the radius R_0 is

$$W = R_0^2\int S_r\sin\theta d\theta d\phi, \quad S_r = \frac{c}{4\pi}E_\theta H\phi.$$

Inserting E_θ and H_ϕ one obtains

$$W = \frac{2e^2\beta^2}{\pi c}\int_0^\infty nJ(\omega)d\omega, \quad J(\omega) = \int_0^\infty q^2\sin\theta d\theta.$$

For $\omega t_0 >> 1$, J can be evaluated in a closed form

$$J = J_{BS} = \frac{1}{\beta^2 n^2}(\ln\frac{1+\beta_n}{|1-\beta_n|} - 2\beta_n) \quad \text{for} \quad \beta_n < 1 \quad \text{and}$$

$$J = J_{BS} + J_{Ch}, \quad J_{Ch} = \frac{\pi\omega t_0}{\beta_n}(1-\frac{1}{\beta_n^2}) \quad \text{for} \quad \beta_n > 1. \qquad (2.4)$$

Tamm identified J_{BS} with the spectral distribution of the bremsstrahlung BS , arising from instant acceleration and deceleration of the charge at the moments $\pm t_0$, resp. On the other hand, J_{Ch} was identified with the spectral distribution of the Čerenkov radiation. This is supported by the fact that

$$W_{Ch} = \frac{2e^2\beta^2}{\pi c}\int_0^\infty nJ_{Ch}(\omega)d\omega = \frac{2e^2\beta^2 t_0}{c}\int_{\beta_n>1}\omega d\omega(1-\frac{1}{\beta_n^2}). \qquad (2.5)$$

strongly resembles the famous Frank-Tamm formula [5] for an infinite medium obtained in a quite different way.

In the absence of dispersion Eqs.(2.3) are easily integrated:

$$H_\phi^T = -\frac{e\beta\sin\theta}{R_0(1-\beta_n\cos\theta)}\{\delta[c_n(t-t_0)-R_0+z_0\cos\theta] - \delta[c_n(t+t_0)-R_0-z_0\cos\theta]\},$$

$$E_\theta^T = -\frac{e\beta\sin\theta}{R_0 n(1-\beta_n\cos\theta)}\{\delta[c_n(t-t_0)-R_0+z_0\cos\theta] - \delta[c_n(t+t_0)-R_0-z_0\cos\theta]\} \quad (2.6).$$

Superscript T means that these expressions originate from Tamm's field strengths (2.2).

3 Comparison with exact solution

3.1 Exact solution

On the other hand, in Ref. [12] there was given an exact solution of the treated problem (i.e., the superluminal charge motion on the finite space interval) in the absence of dispersion. It is assumed that a point charge moves on the interval $(-z_0, z_0)$ lying inside S_0. The charge motion begins at the moment $t = -t_0 = -z_0/v$ and terminates at the moment $t = t_0 = z_0/v$. For convenience we shall refer to the BS shock waves emitted at the beginning of the charge motion ($t = -t_0$) and at its termination ($t = t_0$) as the BS_1 and BS_2 shock waves, resp.

In the wave zone the field strengths are of the form ([12])

$$\vec{E} = \vec{E}_{BS} + \vec{E}_{Ch}, \quad \vec{E}_{BS} = \vec{E}_{BS}^{(1)} + \vec{E}_{BS}^{(2)} \quad \vec{H} = \vec{H}_{BS} + \vec{H}_{Ch},$$

$$\vec{H} = H_\phi\vec{n}_\phi, \quad H_\phi = H_{BS} + H_{Ch}, \quad H_{BS} = H_{BS}^{(1)} + H_{BS}^{(2)}. \qquad (3.1)$$

Here

$$\vec{E}_{BS}^{(1)} = -\frac{e\beta}{n}\frac{\delta[c_n(t+t_0)-r_1]}{\beta_n(z+z_0)-r_1}\frac{r\sin\theta}{r_1}\vec{n}_\theta^{(1)}, \quad \vec{E}_{BS}^{(2)} = \frac{e\beta}{n}\frac{\delta[c_n(t-t_0)-r_2]}{\beta_n(z-z_0)-r_2}\frac{r\sin\theta}{r_2}\vec{n}_\theta^{(2)},$$

$$\vec{E}_{Ch} = \frac{2}{\epsilon r_m\gamma_n}\delta(c_n t - R_m)\Theta(\rho\gamma_n + z_0 - z)\Theta(-\rho\gamma_n + z_0 + z)\vec{n}_m,$$

$$H_{BS}^{(1)} = -e\beta\frac{\delta[c_n(t+t_0)-r_1]}{\beta_n(z+z_0)-r_1}\frac{r\sin\theta}{r_1}, \quad H_{BS}^{(2)} = e\beta\frac{\delta[c_n(t-t_0)-r_2]}{\beta_n(z-z_0)-r_2}\frac{r\sin\theta}{r_2},$$

$$H_{Ch} = \frac{2}{r_m\gamma_n\sqrt{\epsilon\mu}}\delta(c_n t - R_m)\Theta(\rho\gamma_n + z_0 - z)\Theta(-\rho\gamma_n + z_0 + z)\vec{n}_\phi,$$

$$\gamma_n = |1-\beta_n^2|^{-1/2}, \quad r_1 = [(z+z_0)^2+\rho^2]^{1/2}, \quad r_2 = [(z-z_0)^2+\rho^2]^{1/2},$$

$$r_m = [(z-vt)^2 - \rho^2/\gamma_n^2]^{1/2}, \quad R_m = (z+\rho/\gamma_n)/\beta_n,$$

$$n_\theta^{(1)} = [\vec{n}_\rho(z+z_0) - \rho\vec{n}_z]/r_1, \quad n_\theta^{(2)} = [\vec{n}_\rho(z-z_0) - \rho\vec{n}_z]/r_2, \quad \vec{n}_m = (\vec{n}_\rho - n_z/\gamma_n)/\beta_n.$$

The meaning of this notation is as follows: $r = \sqrt{z^2+\rho^2}$ is the distance of the observation point from the origin (it coincides with Tamm's R_0); $r_1 = \sqrt{(z+z_0)^2+\rho^2}$ and $r_2 = \sqrt{(z-z_0)^2+\rho^2}$ are the distances of the observation point from the points of the motion axis where the instant acceleration (at $t = -t_0$) and deceleration (at $t = t_0$) take place. Correspondingly, δ functions $\delta[c_n(t+t_0)-r_1]$ and $\delta[c_n(t-t_0)-r_2]$ describe spherical BS shock waves emitted at these moments; $n_\theta^{(1)}$ and $n_\theta^{(1)}$ are the unit vectors tangent to the above spherical waves and lying in the $\phi = const$ plane; $\vec{E}_{BS}^{(1)}$, $\vec{E}_{BS}^{(2)}$, $\vec{H}_{BS}^{(1)}$ and $\vec{H}_{BS}^{(2)}$ are the electric and magnetic field strengths of the BS shock waves. The function $\delta(c_n t - R_m)$ describes the position of the Čerenkov shock wave (CSW). The inequalities $R_m < c_n t$ and $R_m > c_n t$ correspond to the points lying inside the VC cone and outside it, resp.; $\vec{n}_m$ is the vector lying on the surface of the Vavilov-Čerenkov (VC) cone; r_m is the so-called Čerenkov singularity: $r_m = 0$ on the VC cone surface; $\vec{E}_{Ch}$ and $\vec{H}_{Ch}$ are the electric and magnetic field strengths describing CSW; $\vec{E}_{Ch}$ and $\vec{H}_{Ch}$ are infinite on the surface of the VC cone and vanish outside it. Inside the VC cone $\vec{E}_{Ch}$ and $\vec{H}_{Ch}$ decrease as r^{-2} at large distances and, therefore, do not give contribution in the wave zone where only the radiation terms are essential.

3.2 Comparison with Tamm's solution

At large distances one may develop r_1 and r_2 in (3.1): $r_1 = r + z_0\cos\theta, \quad r_2 = r - z_0\cos\theta$. Here $r = R_0 = [\rho^2 + z^2]^{1/2}$. Neglecting z_0 compared with r in the denominators of $\vec{E}_{BS}$ and $\vec{H}_{BS}$ in (3.1), one gets

$$\vec{E}_T = \vec{E}_{BS}, \quad \vec{H}_T = \vec{H}_{BS}, \quad \vec{E} = \vec{E}_T + \vec{E}_{Ch}, \quad \vec{H} = \vec{H}_T + \vec{H}_{Ch},$$

where $\vec{E}_T$ and $\vec{H}_T$ are the same as in Eq.(2.6). This means that Tamm's field strengths (2.6) decribe only the bremsstrahlung and do not contain the Čerenkov singular terms. Correspondingly, the maxima of their Fourier transforms refer to the BS radiation.
To elucidate why the Čerenkov radiation is absent in Eqs. (2.4), we consider the product of two Θ functions entering into the definition (3.1) of $\vec{E}_{Ch}$ and $\vec{H}_{Ch}$:

$$\Theta(\rho\gamma_n + z_0 - z)\Theta(-\rho\gamma_n + z_0 + z).$$

If for

$$z_0 << \rho\gamma_n - z = r(\gamma_n\sin\theta - \cos\theta) \tag{3.2}$$

one naively neglects the term z_0 inside the Θ functions, the product of two Θ functions reduces to $\Theta(\rho\gamma_n - z)\Theta(-\rho\gamma_n + z)$ that is equal to zero. In this case the Čerenkov radiation drops out.

We prove now that essentially the same approximation was implicitly made during the transition from (2.1) to (2.2). When changing R under the sign of exponent in (2.1) by $R_0 - z'\cos\theta$ it was implicitly assumed that the quadratic term in the development of R is small as compared to the linear one. Consider this more carefully. We develop R up to the second order:

$$R \approx R_0 - z'\cos\theta + \frac{z'^2}{2R}\sin^2\theta.$$

Under the sign of exponent in (2.1) the following terms appear

$$\frac{z'}{v} + \frac{1}{c_n}(R_0 - z'\cos\theta + \frac{z'^2}{2R_0}\sin^2\theta).$$

We collect terms involving z'

$$\frac{z'}{c_n}[(\frac{1}{\beta_n} - \cos\theta) + \frac{z'}{2R_0}\sin^2\theta].$$

Taking for z' its maximal value z_0, we present the condition for the second term in the development of R to be small in the form

$$z_0 << 2R_0(\frac{1}{\beta_n} - \cos\theta)/\sin^2\theta$$

It is seen that the right-hand side of this equation and that of Eq.(3.2) vanish for $\cos\theta = 1/\beta_n$, i.e., at the angle where the Čerenkov radiation exists. This means that the Čerenkov radiation is due to the neglected second-order term in the development of R. Or, in other words, the absence of the Čerenkov radiation in Eqs. (2.5) is due to the omission of second-order terms in the development of R.

3.3 Space distribution of shock waves

Consider space distribution of the electromagnetic field (EMF) at the fixed moment of time. It is convenient to deal with the space distribution of the magnetic vector potential rather than with that of field strengths.
The exact electromagnetic potentials are equal to ([12])

$$\epsilon\Phi = \Phi_1 + \Phi_2 + \Phi_m, \quad \frac{1}{\mu}A_z = \beta\Phi_m.$$

Here

$$\Phi_1 = \frac{e}{r_1}\Theta(r_1 - c_nt - \frac{z_0}{\beta_n}), \quad \Phi_2 = \frac{e}{r_2}\Theta(c_nt - r_2 - \frac{z_0}{\beta_n}),$$

$$\Phi_m = \Phi_m^{(1)} + \Phi_m^{(2)} + \Phi_m^{(3)}, \quad A_z = A_z^{(1)} + A_z^{(2)} + A_z^{(3)}, \tag{3.3}$$

$$A_z^{(1)} = \frac{e\beta}{r_m}\Theta(\rho\gamma_n - z - z_0)\Theta(\frac{z_0}{\beta_n} + r_2 - c_nt)\Theta(c_nt + \frac{z_0}{\beta_n} - r_1),$$

$$A_z^{(2)} = \frac{e\beta}{r_m}\Theta(z - z_0 - \rho\gamma_n)\Theta(r_1 - c_nt - \frac{z_0}{\beta_n})\Theta(c_nt - \frac{z_0}{\beta_n} - r_2),$$

$$A_z^{(3)} = \frac{e\beta}{r_m}\Theta(z_0 + \rho\gamma_n - z)\Theta(z + z_0 - \rho\gamma_n)\Theta(c_nt - R_m)\cdot$$

$$[\Theta(r_1 - c_nt - \frac{z_0}{\beta_n}) + \Theta(\frac{z_0}{\beta_n} + r_2 - c_nt)],$$

(for simplicity we have omitted the μ factor).
Theta functions $\Theta(c_nt + \frac{z_0}{\beta_n} - r_1)$ and $\Theta(r_1 - c_nt - \frac{z_0}{\beta_n})$ define space regions which, correspondingly, have and have not been reached by the the BS_1 shock wave.
Similarly, theta functions $\Theta(c_nt - \frac{z_0}{\beta_n} - r_2)$ and $\Theta(r_2 - c_nt + \frac{z_0}{\beta_n})$ define space regions which correspondingly have and have not been reached by the the BS_2 shock wave.
Finally, theta function $\Theta(c_nt - R_m)$ defines space region that has been reached by the CSW.
The potentials Φ_1 and Φ_2 correspond to the electrostatic fields of the charge resting at $z = -z_0$ up to a moment $-t_0$ and at $z = z_0$ after the moment t_0 whilst Φ_m and A_z describe the field of a moving charge. Schematic representation of the shock waves position at the fixed moment of time is shown in Fig. 1. In the space regions 1 and 2 corresponding to $z < \rho\gamma_n - z_0$ and $z > \rho\gamma_n + z_0$, resp., there are observed only BS shock waves. In the space region 1, at the fixed observation point the BS_1 shock wave (defined by $c_nt + z_0/\beta_n = r_1$) arrives first and BS_2 wave (defined by $c_nt - z_0/\beta_n = r_2$) later. In the space region 2, these waves arrive in the reverse order. In the space region 3, defined by $\rho\gamma_n - z_0 < z < \rho\gamma_n + z_0$, there are BS_1, BS_2 and CSW defined by the equation $c_nt = R_m$. Before the arrival of the CSW (i.e., for $R_m > c_nt$) there is an electrostatic field of a charge resting at $z = -z_0$. After the arrival of the last of the BS shock waves there is an electrostatic field of a charge resting at $z = z_0$. The space region, where Φ_m (and, therefore, the field of a moving charge) differs from zero, lies between the BS_1 and BS_2 shock waves in the regions 1 and 2 and between CSW and one of the BS shock waves in the region 3 (for details see Ref. [12]). Space region 3 in its turn consists of two subregions 3_1 and 3_2 defined by the equations $\rho\gamma_n - z_0 < z < (\rho^2\gamma_n^2 + z_0^2/\beta_n^2)^{1/2}$ and $(\rho^2\gamma_n^2 + z_0^2/\beta_n^2)^{1/2} < z < \rho\gamma_n + z_0$, resp. In the region 3_1 at first there arrive CSW, then

BS_1 and, finally, BS_2. In region 3_2 two last waves arrive in the reverse order.
The polarization vectors of bremsstrahlungs are tangential to the spheres BS_1 and BS_2 and lie in the $\phi = const$ plane coinciding with the plane of Fig.1. They are directed along the unit vectors $\vec{n}_\theta^{(1)}$ and $\vec{n}_\theta^{(2)}$, resp. The polarization vector of CSW (directed along $\vec{n}_m$) lies on the CSW. It is shown by the solid line in Fig.1 and also lies in the $\phi = const$ plane. The magnetic field having only the ϕ nonvanishing component is normal to the plane of figure. The Poynting vectors defining the direction of the energy transfer are normal to BS_1, BS_2 and CSW, resp.
The Čerenkov radiation in the (ρ, z) plane differs from zero inside the narrow beam of the width $2z_0 \sin\theta_c$, where θ_c is the inclination of the beam towards the motion axis ($\cos\theta_c = 1/\beta_n$). When the charge velocity tends to the velocity of light in medium, the width of the above beam as well as the inclination angle tend to zero. That is, in this case the beam propagates in a nearly forward direction.

3.4 Time evolution of the electromagnetic field on the sphere surface

Consider the distribution of VP (in units e/R_0) on the sphere S_0 of the radius R_0 at different moments of time. There is no EMF on S_0 up to a moment $T_n = 1 - \epsilon_0(1 + 1/\beta_n)$. Here $T_n = c_n t/R_0$. In the time interval

$$1 - \epsilon_0(1 + \frac{1}{\beta_n}) \le T_n \le 1 - \epsilon_0(1 - \frac{1}{\beta_n}) \tag{3.4}$$

BS radiation begins to fill the back part of S_0 corresponding to the angles

$$-1 < \cos\theta < \frac{1}{2\epsilon_0}[(T_n + \frac{\epsilon_0}{\beta_n})^2 - 1 - \epsilon_0^2] \tag{3.5}$$

(Fig. 2, curve 1). In the time interval

$$1 - \epsilon_0(1 - \frac{1}{\beta_n}) \le T_n \le [1 - (\frac{\epsilon_0}{\beta_n\gamma_n})^2]^{1/2} \tag{3.6}$$

BS radiation begins to fill the front part of S_0 as well:

$$\frac{1}{2\epsilon_0}[1 + \epsilon_0^2 - (T_n - \frac{\epsilon_0}{\beta_n})^2] \le \cos\theta \le 1.$$

The illuminated back part of S_0 is still given by (3.5) (Fig. 2, curve 2). The finite jumps of VP shown in these figures lead to the δ-type singularities in Eqs. (3.1) defining BS electromagnetic strengths. In the time intervals (3.4) and (3.6) these jumps have a finite height. The vector potential is maximal at the angle at which the jump occurs. The height of the BS shock wave jump and the value of VP tend to infinity at the angles

$$\cos\theta_1 = -\frac{\epsilon_0}{\beta_n^2\gamma_n^2} + \frac{1}{\beta_n}[1 - (\frac{\epsilon_0}{\beta_n\gamma_n})^2]^{1/2} \quad \text{and} \quad \cos\theta_2 = \frac{\epsilon_0}{\beta_n^2\gamma_n^2} + \frac{1}{\beta_n}[1 - (\frac{\epsilon_0}{\beta_n\gamma_n})^2]^{1/2}. \tag{3.7}$$

which are reached at the time

$$T_{Ch} = \frac{c_n t_{Ch}}{R_0} = [1 - (\frac{\epsilon_0}{\beta_n\gamma_n})^2]^{1/2}$$

(Fig. 2, curve 3) and correspond to the intersection of S_0 by the lines $z = \rho\gamma_n - z_0$ and $z = \rho\gamma_n + z_0$, resp. (Fig.1). At this moment the illuminated front and back parts of S_0 are given by $-1 < \cos\theta < \cos\theta_1$ and $\cos\theta_2 < \cos\theta < 1$, resp. At the moment $t = t_{Ch}$ the Čerenkov shock wave intersects S_0 at the angles θ_1 and θ_2.
Beginning from this moment, the CSW intersects the sphere S_0 at the angles

$$\cos\theta = \frac{T_n}{\beta_n} - \frac{1}{\beta_n\gamma_n}(1 - T_n^2)^{1/2} \quad \text{and} \quad \cos\theta = \frac{T_n}{\beta_n} + \frac{1}{\beta_n\gamma_n}(1 - T_n^2)^{1/2}.$$

The positions of the BS_1 and BS_2 shock waves are given by

$$\cos\theta = \frac{1}{2\epsilon_0}[(T_n + \frac{\epsilon_0}{\beta_n})^2 - 1 - \epsilon_0^2] \quad \text{and} \quad \cos\theta = \frac{1}{2\epsilon_0}[1 + \epsilon_0^2 - (T_n - \frac{\epsilon_0}{\beta_n})^2],$$

respectively (i.e., BS shock waves follow after CSW). Therefore, at this moment BS fills the angle regions

$$-1 \le \cos\theta \le \frac{1}{2\epsilon_0}[(T_n + \frac{\epsilon_0}{\beta_n})^2 - 1 - \epsilon_0^2] \quad \text{and}$$

$$\frac{1}{2\epsilon_0}[1 + \epsilon_0^2 - (T_n - \frac{\epsilon_0}{\beta_n})^2] \le \cos\theta \le 1,$$

while VC radiation occupies the angle interval

$$\cos\theta_1 \le \cos\theta \le \frac{T_n}{\beta_n} - \frac{1}{\beta_n\gamma_n}(1 - T_n^2)^{1/2} \quad \text{and} \quad \frac{T_n}{\beta_n} + \frac{1}{\beta_n\gamma_n}(1 - T_n^2)^{1/2} \le \cos\theta \le \cos\theta_2.$$

Therefore, VC radiation field and BS overlap in the regions

$$\frac{1}{2\epsilon_0}[(T_n + \frac{\epsilon_0}{\beta_n})^2 - 1 - \epsilon_0^2] \le \cos\theta \le \frac{T_n}{\beta_n} - \frac{1}{\beta_n\gamma_n}(1 - T_n^2)^{1/2} \quad \text{and}$$

$$\frac{T_n}{\beta_n} + \frac{1}{\beta_n\gamma_n}(1 - T_n^2)^{1/2} \le \cos\theta \le \frac{1}{2\epsilon_0}[1 + \epsilon_0^2 - (T_n - \frac{\epsilon_0}{\beta_n})^2]$$

BS_1 and BS_2 have finite jumps in this angle interval (Fig. 3). The non-illuminated part of S_0 is

$$\frac{T_n}{\beta_n} - \frac{1}{\beta_n\gamma_n}(1 - T_n^2)^{1/2} \le cos\theta \le \frac{T_n}{\beta_n} + \frac{1}{\beta_n\gamma_n}(1 - T_n^2)^{1/2}.$$

This lasts up to a moment $T_n = 1$ when the Čerenkov shock wave intersects S_0 only once at the point corresponding to the angle $\cos\theta = 1/\beta_n$ (Fig. 4). The positions of the BS_1 and BS_2 shock waves at the moment $T_n = 1$ are given by

$$\cos\theta = \frac{1}{\beta_n} - \frac{\epsilon_0}{2\beta_n^2\gamma_n^2} \quad \text{and} \quad \cos\theta = \frac{1}{\beta_n} + \frac{\epsilon_0}{2\beta_n^2\gamma_n^2},$$

resp. Again, the jumps of BS waves have finite heights while the Čerenkov potentials (and field strengths) are infinite at the angle $\cos\theta = 1/\beta_n$ where CSW intersects S_0. After the moment $T_n = 1$, CSW leaves S_0. However, the Čerenkov post-action still remains (Fig. 5). At the subsequent moments of time the BS_1 and BS_2 shock waves approach each other. They meet at the moment

$$T_n = [1 + (\frac{\epsilon_0}{\beta_n\gamma_n})^2]^{1/2}. \tag{3.8}$$

The corresponding angle is

$$\cos\theta = \frac{1}{\beta_n}[1 + (\frac{\epsilon_0}{\beta_n\gamma_n})^2]^{1/2}.$$

After this moment BS shock waves pass through each other and begin to go away from each other (Fig. 6). Now BS_1 and BS_2 move along the front and back semi-spheres, resp. There is no EMF on the part of S_0 lying between them. The illuminated parts of S_0 are now given by

$$-1 \le \cos\theta \le \frac{1}{2\epsilon_0}[1 + \epsilon_0^2 - (T_n - \frac{\epsilon_0}{\beta_n})^2] \quad \text{and} \quad \frac{1}{2\epsilon_0}[(T_n + \frac{\epsilon_0}{\beta_n})^2 - 1 - \epsilon_0^2] \le \cos\theta \le 1.$$

The electromagnetic field is zero inside the angle interval

$$\frac{1}{2\epsilon_0}[1 + \epsilon_0^2 - (T_n - \frac{\epsilon_0}{\beta_n})^2] \le \cos\theta \le \frac{1}{2\epsilon_0}[(T_n + \frac{\epsilon_0}{\beta_n})^2 - 1 - \epsilon_0^2]$$

After the moment of time (3.8) BS_1 and BS_2 may occupy the same angular positions $cos\theta_2$ and $cos\theta_1$ like BS_2 and BS_1 shown in Fig. 2. But now their jumps are finite. After the moment

$$T_n = 1 + \epsilon_0(1 - \frac{1}{\beta_n})$$

the front part of S_0 begins not to be illuminated (Fig. 7). The illuminated back part of S_0 is given by

$$-1 \le \cos\theta \le -1 + \frac{2(1+\epsilon_0)}{\beta_n} - \frac{2\epsilon_0}{\beta_n^2}.$$

In the subsequent time the illuminated part of S_0 is given by

$$-1 \le \cos\theta \le \frac{1}{2\epsilon_0}[1 + \epsilon_0^2 - (T_n - \frac{\epsilon_0}{\beta_n})^2]$$

As time goes, the illuminated part of S_0 diminishes. Finally , after the moment

$$T_n = 1 + \epsilon_0(1 + \frac{1}{\beta_n})$$

the EMF radiation leaves the surface of S_0 (and its interior).
For small $\epsilon_0 = z_0/R_0$ the Čerenkov singular radiation occupies the angular region

$$\frac{1}{\beta_n} - \frac{\epsilon_0}{\beta_n^2\gamma_n^2} \le \cos\theta \le \frac{1}{\beta_n} + \frac{\epsilon_0}{\beta_n^2\gamma_n^2},$$

while BS is infinite at the boundary points of this interval (i.e., at $\cos\theta = \frac{1}{\beta_n} \pm \frac{\epsilon_0}{\beta_n^2\gamma_n^2}$).
In the opposite case ($\epsilon_0 \approx 1$) the singular Čerenkov radiation field is confined to the angular region

$$\frac{2}{\beta_n^2} - 1 \le \cos\theta \le 1,$$

while BS has singularities at $\cos\theta = \frac{2}{\beta_n^2} - 1$, and $\cos\theta = 1$.

We summarize here main differences between Čerenkov radiation and bremsstrahlung: On the sphere S_0 VC radiation occupies the angular region

$$\cos\theta_1 \le \cos\theta \le \cos\theta_2,$$

where θ_1 and θ_2 are given by Eq. (3.7). At each particular moment of time T_n in the interval

$$[1 - (\frac{\epsilon_0}{\beta_n\gamma_n})^2]^{1/2} \le T_n \le 1$$

the VC electromagnetic potentials and field strengths are infinite at the angles

$$\cos\theta = \frac{T_n}{\beta_n} - \frac{1}{\beta_n\gamma_n}\sqrt{1 - T_n^2} \quad \text{and} \quad \cos\theta = \frac{T_n}{\beta_n} + \frac{1}{\beta_n\gamma_n}\sqrt{1 - T_n^2}.$$

After the moment $T_n = 1$ the Čerenkov singularities leave the sphere S_0, but the Čerenkov post-action still remains. This lasts up to the moment $T_n = [1 + (\frac{\epsilon_0}{\beta_n\gamma_n})^2]^{1/2}$.
On the other hand, BS runs over all the sphere S_0 in the time interval

$$1 - \epsilon_0(1 + \frac{1}{\beta_n}) \le T_n \le 1 + \epsilon_0(1 + \frac{1}{\beta_n}).$$

The vector potential of BS is infinite only at the angles θ_1 and θ_2 at the particular moment of time $T_n = \sqrt{1 - \epsilon_0^2/\beta_n^2\gamma_n^2}$. For other times the VP of BS exhibits finite jumps in the angle interval $-\pi \le \theta \le \pi$. The BS electromagnetic field strengths are infinite at those angles. Therefore, Čerenkov singularities of the vector potential run over the region $\cos\theta_1 \le \cos\theta \le \cos\theta_2$ of the sphere S_0, while the BS vector potential is infinite only at the angles θ_1 and θ_2 where BS shock waves meet CSW.

3.5 Comparison with Tamm's vector potential

Now we evaluate Tamm's VP

$$A_T = \int_{-\infty}^{\infty} d\omega \exp(i\omega t) A_\omega$$

Substituting here A_ω given by (2.1), we get in the absence of dispersion

$$A_T = \frac{e\beta}{R}\Theta[\epsilon_0 - (T_n - 1)/(\frac{1}{\beta_n} - \cos\theta)] \cdot \Theta[\epsilon_0 + (T_n - 1)/(\frac{1}{\beta_n} - \cos\theta)]. \qquad (3.9)$$

Here $R = \{[z(1 - \beta_n\cos\theta) - vt + R_0\beta_n]^2 + \rho^2(1 - \beta_n\cos\theta)^2\}^{1/2}$.
This VP is obtained also from A_z given by (3.3) if we leave in it the terms $A_z^{(1)}$ and $A_z^{(2)}$ describing BS in the regions 1 and 2 (see Fig.1) (with omitting z_0 in the factors $\Theta(\rho\gamma_n - z - z_0)$ and $\Theta(z - z_0 - \rho\gamma_n)$ entering into them) and drop the term $A_z^{(3)}$ which is responsible (as we have learned from the previous section) for the VC radiation and BS in region 3 and which vanishes for $\epsilon_0 = 0$. It is seen at once that A_z is infinite only at

$$T_n = 1, \quad \cos\theta = 1/\beta_n. \qquad (3.10)$$

This may be compared with the exact consideration of the previous section which shows that the BS part of A_z is infinite at the moment

$$T_{Ch} = \frac{c_n t_{Ch}}{R_0} = [1 - (\frac{\epsilon_0}{\beta_n \gamma_n})^2]^{1/2} \tag{3.11}$$

at the angles $\cos\theta_1$ and $\cos\theta_2$ defined by (3.7). It is seen that Eq.(3.11), $\cos\theta_1$ and $\cos\theta_2$ transform into (3.9) when $\epsilon_0 \to 0$. Due to the dropping of the $A_z^{(3)}$ term in (3.3) and the omission of terms containing ϵ_0 in $\cos\theta_1$ and $\cos\theta_2$, BS_1 and BS_2 waves have now the common infinite maximum at $\cos\theta = 1/\beta_n$.

The analysis of (3.9) shows that Tamm's VP is distributed over S_0 in the following way. There is no EMF of the moving charge up to the moment $T_n = 1 - \epsilon_0(1 + 1/\beta_n)$. For

$$1 - \epsilon_0(1 + \frac{1}{\beta_n}) < T_n < 1 - \epsilon_0(1 - \frac{1}{\beta_n})$$

EMF fills only the back part of S_0,

$$-1 < \cos\theta < \frac{1}{\beta_n} - \frac{1}{\epsilon_0}(1 - T_n)$$

(Fig. 8, curve 1). In the time interval

$$1 - \epsilon_0(1 - \frac{1}{\beta_n}) < T_n < 1 + \epsilon_0(1 - \frac{1}{\beta_n})$$

the illuminated parts of S_0 are given by

$$-1 < \cos\theta < \frac{1}{\beta_n} - \frac{1}{\epsilon_0}(1 - T_n) \quad \text{and} \quad \frac{1}{\beta_n} + \frac{1}{\epsilon_0}(1 - T_n) < \cos\theta < 1$$

(Fig. 8, curves 2 and 3). The jumps of the BS_1 and BS_2 shock waves are finite. As T_n tends to 1, the BS_1 and BS_2 shock waves approach each other and fuse at $T_n = 1$. Tamm' VP is infinite at this moment at the angle $\cos\theta = 1/\beta_n$ (Fig. 9). For

$$1 < T_n < 1 + \epsilon_0(1 - \frac{1}{\beta_n})$$

the BS shock waves pass through each other and begin to go away from each other, BS_1 and BS_2 filling the front and back parts of S_0, resp. (Fig. 10):

$$\frac{1}{\beta_n} + \frac{1}{\epsilon_0}(T_n - 1) < \cos\theta < 1 \quad (BS_1) \quad \text{and}$$

$$-1 < \cos\theta < \frac{1}{\beta_n} - \frac{1}{\epsilon_0}(T_n - 1) \quad (BS_2).$$

For larger times

$$1 + \epsilon_0(1 - \frac{1}{\beta_n}) < T_n < 1 + \epsilon_0(1 + \frac{1}{\beta_n})$$

only back part of S_0 is illumihated:

$$-1 < \cos\theta < \frac{1}{\beta_n} - \frac{1}{\epsilon_0}(T_n - 1) \quad (BS_2).$$

Finally, for $T_n > 1 + \epsilon_0(1 + 1/\beta_n)$ there is no radiation field on S_0 and inside it.
Roughly speaking, Tamm's vector potential (3.9) describing evolution of BS shock waves in the absence of CSW imitates it in the neighbourhood of $\cos\theta = 1/\beta_n$.

4 Quantum analysis of Tamm's formula

We turn now to the quantum consideration of Tamm's formula. The usual approach proceeds as follows [16]. Consider the uniform rectilinear (say, along the z axis) motion of a point charged particle with the velocity v. The conservation of energy-momentum is written as

$$\vec{p} = \vec{p}' + \hbar\vec{k}, \quad \mathcal{E} = \mathcal{E}' + \hbar\omega, \tag{4.1}$$

where $\vec{p}$,$\mathcal{E}$ and $\vec{p}'$,$\mathcal{E}'$ are the 3- momentum and energy of the initial and final states of the moving charge; $\hbar\vec{k}$ and $\hbar\omega$ are the 3-momentum and energy of the emitted photon. We present (4.1) in the 4-dimensional form

$$p - \hbar k = p', \quad p = (\vec{p}, \mathcal{E}/c). \tag{4.2}$$

Squaring both sides of this equation and taking into account that $p^2 = p'^2 = -m^2c^2$ (m is the rest mass of a moving charge), one gets

$$(pk) = \hbar k^2/2, \quad k = (\vec{k}, k_0), \quad k_0 = \omega/c. \tag{4.3}$$

Or, in a more manifest form

$$\cos\theta_k = \frac{1}{\beta_n}(1 + \frac{n^2 - 1}{2}\frac{\hbar\omega}{\mathcal{E}}). \tag{4.4}$$

Here $\beta_n = v/c_n$, $c_n = c/n$ is the light velocity in medium, n is its refractive index. When deriving (4.4) it was implicitly suggested that the absolute value of photon 3- momentum and its energy are related by the Minkowski formula: $|\vec{k}| = \omega/c_n$.
When the energy of the emitted Čerenkov photon is much smaller than the energy of a moving charge, Eq.(4.4) reduces to

$$\cos\theta_k = 1/\beta_n, \tag{4.5}$$

which can be written in a manifestly covariant form

$$(pk) = 0. \tag{4.6}$$

Up to now we suggested that the emitted photon has definite energy and momentum. The wave function of a photon propagating in vacuum [17] and medium look alike

$$iN\vec{e}\exp[i(\vec{k}\vec{r} - \omega t)], \quad (\vec{e}\vec{k}) = 0, \quad \vec{e}^2 = 1, \tag{4.7}$$

where $|\vec{k}| = \omega/c$ and $|\vec{k}| = \omega/c_n$ for the motion in vacuum and medium, resp., N is the real normalization constant and $\vec{e}$ is the photon polarization vector lying in the plane passing through $\vec{k}$ and $\vec{p}$:

$$\vec{e}_\rho = -\cos\theta_k, \quad \vec{e}_z = \sin\theta_k, \quad \vec{e}_\phi = 0, \quad (ek) = 0. \tag{4.8}$$

The photon wave function (4.7) identified with the classical vector potential is obtained in the following way. We take the positive-frequency part of the second-quantized vector potential operator and apply it to the coherent state with the fixed $\vec{k}$. The eigenvalue

of this VP operator is just (4.7). Below we show that gauge invariance permits one to present a wave function in the form having the form of a classical vector potential

$$iN' p_\mu \exp(ikx), \quad (pk) = 0. \tag{4.9}$$

where N' is another real constant. Now we take into account that photons described by the wave function (4.7) are created by the axially symmetric current of a moving charge. According to Glauber ([18], Lecture 3), to obtain VP in the coordinate representation, one should make superposition of the wave functions (4.7) by taking into account the relation (4.6) which tells us that that photon is emitted at the Čerenkov angle θ_k defined by (4.5). This superposition is given by

$$A_\mu(x) = iN' \int p_\mu \exp(ikx)\delta(pk) d^3k/\omega.$$

The factor $1/\omega$ is introduced using the analogy with the photon wave function in vacuum where it is needed for the relativistic covariance of A_μ. The expression $p_\mu\delta(pu)$ is (up to non-essential factor) the Fourier transform of the classical current of the uniformly moving charge. This current creates photons in coherent states which are observed experimentally. In particular, they are manifested as a classical electromagnetic radiation. We rewrite A_μ in a slightly extended form

$$A_\mu = iN' \int p_\mu \exp[i(\vec{kr} - \omega t)]\delta[\frac{\mathcal{E}\omega}{c^2}(1 - \beta_n \cos\theta)]\frac{n^3}{c^3} d\phi d\cos\theta\omega d\omega. \tag{4.10}$$

Introducing the cylindrical coordinates ($\vec{r} = \rho\vec{n}_\rho + z\vec{n}_z$), we present $\vec{kr}$ in the form

$$\vec{kr} = \frac{\omega}{c_n}[\rho\sin\theta\cos(\phi - \phi_r) + z\cos\theta].$$

Inserting this into (4.10) we get

$$A_\mu(\vec{r}, t) = iN'' \int p_\mu \exp[i\omega(\frac{z}{c_n}\cos\theta_k - t)] \exp[\frac{i\omega}{c_n}\rho\sin\theta_k\cos(\phi - \phi_r)] d\phi d\omega,$$

where N'' is the real modified normalization constant and ϕ_r is the azimuthal angle in the usual space. Integrating over ϕ one gets

$$A_0(\vec{r}, t) = A_z(\vec{r}, t)/\beta, \quad A_z(\vec{r}, t) = \int_0^\infty \exp(-i\omega t) A_z(\vec{r}, \omega) d\omega,$$

where

$$A_z(\vec{r}, \omega) = \frac{2\pi i N''}{\sin\theta_k} \exp(\frac{i\omega}{c_n}\cos\theta_k z) J_0(\frac{\omega}{c_n}\rho\sin\theta_k). \tag{4.11}$$

We see that $A_z(\vec{r}, \omega)$ is the oscillating function of the frequency ω without a pronounced δ- type maximum. In the $\vec{r}, t$ representation $A_z(\vec{r}, t)$ (and, therefore, photon's wave function) is singular on the Čerenkov cone $vt - z = \rho/\gamma_n$

$$ReA_z = 2\pi N'' p_z \int \sin\omega(t - z/v) J_0(\frac{\omega\rho}{c_n}\sin\theta_k) d\omega =$$

$$= 2\pi N'' p_z \frac{v}{[(z - vt)^2 - \rho^2/\gamma_n^2]^{1/2}} \Theta((z - vt)^2 - \rho^2/\gamma_n^2),$$

$$ImA_z = 2\pi N'' p_z \int \cos\omega(t - z/v) J_0(\frac{\omega\rho}{c_n}\sin\theta_k) d\omega =$$

$$= 2\pi N'' p_z \frac{v}{[\rho^2/\gamma_n^2 - (z - vt)^2]^{1/2}} \Theta(\rho^2/\gamma_n^2 - (z - vt)^2)$$

Despite the fact that the wave function (5.10) satisfies free wave equation and does not contain singular Neumann functions N_0 (needed to satisfy Maxwell equations with a moving charge current in their r.h.s.), its real part (which, roughly speaking, corresponds to the classic electromagnetic potential) properly describes the main features of the VC radiation.

4.1 Choice of polarization vector

The Maxwell equations in medium with the constant ϵ and μ are given by

$$div\vec{B} = 0, \quad curl\vec{E} = -\frac{1}{c}\frac{\partial\vec{B}}{\partial t},$$

$$div\vec{D} = 4\pi\rho, \quad curl\vec{H} = \frac{1}{c}\frac{\partial\vec{D}}{\partial t} + \frac{4\pi}{c}\vec{j},$$

$$\vec{D} = \epsilon\vec{E}, \quad \vec{B} = \mu\vec{H}.$$

The first two Maxwell equations are satisfied if we put

$$\vec{B} = curl\vec{A}, \quad \vec{E} = -\nabla\Phi - \frac{1}{c}\dot{\vec{A}}.$$

Then, two other equations give equations for $\vec{A}$ and Φ

$$(\Delta - \frac{1}{c_n^2}\frac{\partial^2}{\partial t^2})\vec{A} = -\frac{4\pi\mu}{c}\vec{j}, \quad (\Delta - \frac{1}{c_n^2}\frac{\partial^2}{\partial t^2})\Phi = -\frac{4\pi}{\epsilon}\rho.$$

These electromagnetic potentials meet the following gauge condition:

$$div\vec{A} + \frac{\varepsilon\mu}{c}\frac{\partial\Phi}{\partial t} = 0.$$

We apply the gauge transformation

$$\vec{A} \to \vec{A}' = \vec{A} + \nabla\chi, \quad \Phi \to \Phi' = \Phi - \frac{1}{c}\dot{\chi}.$$

to the vector potential (4.7) which plays the role of the photon wave function. We chose the generating function χ in the form

$$\chi = \alpha\exp[i(\vec{kr} - \omega t)],$$

where α will be determined later. Thus,

$$\vec{A}' = (N\vec{e} + i\alpha\vec{k})\exp[i(\vec{kr} - \omega t)], \quad \Phi' = i\omega\alpha/c\exp[i(\vec{kr} - \omega t)],$$

where $\vec{e}$ is given by (4.8). We require the disappearance of the ρ component of $\vec{A}'$. This fixes α:

$$\alpha = \frac{N}{ik}\cot\theta_k.$$

The nonvanishing components of $\vec{A}'$ are given by

$$A'_z = \frac{N}{\sin\theta_k}\exp\left[i(\vec{kr} - \omega t)\right], \quad A'_0 = \frac{N}{n}\cot\theta_k \exp\left[i(\vec{kr} - \omega t)\right].$$

It is easy to see that $A'_z = \beta A'_0$. This completes the proof of (4.9).

5 Space distribution of Fourier components

The Fourier transform of the vector potential on the sphere S_0 of the radius R_0 is given by

$$ReA_\omega = \frac{e}{2\pi c}\int_{-\epsilon_0}^{\epsilon_0}\frac{dz}{Z}\cos[\frac{R_0\omega}{c_n}(\frac{z}{\beta_n} + Z)],$$

$$ImA_\omega = -\frac{e}{2\pi c}\int_{-\epsilon_0}^{\epsilon_0}\frac{dz}{Z}\sin[\frac{R_0\omega}{c_n}(\frac{z}{\beta_n} + Z)] \qquad (5.1).$$

Here $Z = (1 + z^2 - 2z\cos\theta)^{1/2}$. For $z_0 << R_0$ these expressions should be compared with the real and imaginary parts of Tamm's approximate VP (2.2):

$$ReA_\omega = \frac{e\beta q}{\pi R_0\omega}\cos(\frac{\omega R_0}{c_n}), \quad ImA_\omega = -\frac{e\beta q}{\pi R_0\omega}\sin(\frac{\omega R_0}{c_n}). \qquad (5.2)$$

These quantities are evaluated (in units $e/2\pi c$) for

$$\frac{\omega R_0}{c_n} = 100, \quad \beta = 0.99, \quad n = 1.334, \quad \epsilon_0 = 0.1$$

(see Figs. 11, 12). We observe that angular distributions of VPs (5.1) and (5.2) practically coincide having maxima on the small part of S_0 in the neighbourhood of $\cos\theta = 1/\beta_n$. It is this minor difference between (5.1) and (5.2) that is responsible for the Čerenkov radiation which is described only by Eq. (5.1).

Now we evaluate the angular dependence of VP (5.1) on the sphere S_0 for the case when z_0 practically coincides with R_0 ($\epsilon = 0.98$). Other parameters remain the same. We see (Fig. 13) that angular distribution fills the whole sphere S_0. There is no pronounced maximum in the vicinity of $\cos\theta = 1/\beta_n$.

We cannot extend these results to larger z_0 as the motion interval will partly lie outside S_0. To consider a charge motion on an arbitrary finite interval, we evaluate the distribution of VP on the cylinder surface C co-axial with the motion axis. Let the radius of this cylinder be ρ. Making the change of variables $z' = z + \rho\sinh\chi$ under the sign of integral in (2.1), one obtains

$$ReA_\omega = \frac{e}{2\pi c}\int_{\chi_1}^{\chi_2}\cos[\frac{\omega\rho}{c}(\frac{z}{\rho\beta} + \frac{1}{\beta}\sinh\chi + n\cosh\chi)]d\chi,$$

$$ImA_\omega = -\frac{e}{2\pi c}\int_{\chi_1}^{\chi_2}\sin[\frac{\omega\rho}{c}(\frac{z}{\rho\beta} + \frac{1}{\beta}\sinh\chi + n\cosh\chi)]d\chi, \qquad (5.3)$$

where $\sinh\chi_1 = -(z_0 + z)/\rho$, $\sinh\chi_2 = (z_0 - z)/\rho$.

The distributions of ReA_ω and ImA_ω (in units $e/2\pi c$) on the surface C as function of $\tilde{z} = z/\rho$ are shown in Figs 14-17 for different values of $\epsilon_0 = z_0/\rho$ and ρ fixed. The calculations were made for $\beta = 0.99$ and $\omega\rho/c = 100$. We observe that for small ϵ_0 the electromagnetic field differs from zero only in the vicinity $\tilde{z} = \gamma_n$, which corresponds to $\cos\theta = 1/\beta_n$ (Figs. 14 and 15). As ϵ_0 increases, the VP begin to diffuse over the cylinder surface. This is illustrated in Figs. 16 and 17 where only the real parts of A_ω for $\epsilon_0 = 1$ and $\epsilon_0 = 10$ are presented (as the behaviour of ReA_ω and ImA_ω is very much alike (Figs. 14 and 15 clearly demonstrate this), we limit ourselves to the consideration of ReA_ω). We observe the disappearance of pronounced maxima at $\cos\theta = 1/\beta_n$. For the infinite motion ($z_0 \to \infty$) Eqs. (5.3) reduce to

$$ReA_\omega = \frac{e}{2\pi c}\int_{-\infty}^{\infty}\cos[\frac{\omega\rho}{c}(\frac{z}{\rho\beta} + \frac{1}{\beta}\sinh\chi + n\cosh\chi)]d\chi,$$

$$ImA_\omega = -\frac{e}{2\pi c}\int_{-\infty}^{\infty}\sin[\frac{\omega\rho}{c}(\frac{z}{\rho\beta} + \frac{1}{\beta}\sinh\chi + n\cosh\chi)]d\chi \qquad (5.4)$$

These expressions can be evaluated in the analytical form (see Appendix)

$$\frac{ReA_\omega}{e/2\pi c} = -\pi[J_0(\frac{\omega\rho}{v\gamma_n})\sin(\frac{\omega z}{v}) + N_0(\frac{\omega\rho}{v\gamma_n})\cos(\frac{\omega z}{v})],$$

$$\frac{ImA_\omega}{e/2\pi c} = \pi[N_0(\frac{\omega\rho}{v\gamma_n})\sin(\frac{\omega z}{v}) - J_0(\frac{\omega\rho}{v\gamma_n})\cos(\frac{\omega z}{v})] \qquad (5.5)$$

for $v > c_n$ and

$$\frac{ReA_\omega}{e/2\pi c} = 2\cos(\frac{\omega z}{v})K_0(\frac{\rho\omega}{v\gamma_n}), \quad \frac{ImA_\omega}{e/2\pi c} = -2\sin(\frac{\omega z}{v})K_0(\frac{\rho\omega}{v\gamma_n}) \qquad (5.6)$$

for $v < c_n$ (remember that $\gamma_n = |1 - \beta_n^2|^{-1/2}$). We see that for the infinite charge motion the Fourier transform A_ω is a pure periodical function of z (and, therefore, of the angle θ). This assertion does not depend on the ρ and ω values. For example, for $\omega\rho/v\gamma_n >> 1$ one gets

$$\frac{ReA_\omega}{e/2\pi c} = -\sqrt{\frac{2v\pi\gamma_n}{\rho\omega}}\sin[\frac{\omega}{v}(z + \frac{\rho}{\gamma_n}) - \frac{\pi}{4}], \quad \frac{ImA_\omega}{e/2\pi c} = -\sqrt{\frac{2v\pi\gamma_n}{\rho\omega}}\cos[\frac{\omega}{v}(z + \frac{\rho}{\gamma_n}) - \frac{\pi}{4}]$$

for $v > c_n$ and

$$\frac{ReA_\omega}{e/2\pi c} = \sqrt{\frac{2v\pi\gamma_n}{\rho\omega}}\cos(\frac{\omega z}{v})\exp(-\frac{\rho\omega}{v\gamma_n}), \quad \frac{ImA_\omega}{e/2\pi c} = -\sqrt{\frac{2v\pi\gamma_n}{\rho\omega}}\sin(\frac{\omega z}{v})\exp(-\frac{\rho\omega}{v\gamma_n})$$

for $v < c_n$.

In Fig. 18, by comparing the real part of A_ω evaluated according to Eq.(5.4) with the analytical expression (5.5) we observe their perfect agreement on the small interval

of cylinder C surface (they are indistinguished on the treated interval). The same coincidence is valid for ImA_ω.
The absence of pronounced maxima of potentials and field strengths for the charge motion on the finite interval may qualitatively be understood as follows. We begin with the exact equations (3.1) and (3.3) for the field strengths and potentials in the space-time representation. Making inverse Fourier transform from them, we arrive at Eqs. (5.1)-(5.5) of this section. Now, if the charge motion takes place on the small space interval, field strengths and potentials (3.1) and (3.3) have singularities on a rather small space-time interval (as the Čerenkov beam is thin in this case). Therefore, Fourier transforms of (3.1) and (3.3) should be different from zero in the limited space region. For the charge motion on a large interval field strengths and potentials (3.1) and (3.3) have singularities in a larger space-time domain (as the Čerenkov beam is rather broad now). Consequently, Fourier transforms of (3.1) and (3.3) should be different from zero in a larger space region.
By comparing (5.4) with (5.5) and (5.6) we recover integrals which, to the best of our knowledge are absent in the mathematical literature (see Appendix).

6 Discussion

So far, our conclusion on the absence of a Čerenkov radiation in Eqs.(2.2) and (2.3) was proved only for the dispersion-free case (as only in this case we have exact solution). At this moment we are unable to prove the same result in the general case with dispersion. We see that Tamm's formulae describe evolution and interference of two BS shock waves emitted at the beginning and at the end of the charge motion and do not contain the Čerenkov radiation.

Now the paradoxical results of Refs. [10,11], where the Tamm's formulae were investigated numerically become understandable. Their authors attributed the term J_{Ch} in Eqs. (2.4) to the interference of the bremsstrahlung shock waves emitted at the moments of instant acceleration and deceleration. Without knowing that Čerenkov radiation is absent in Tamm's equations (2.2) they concluded that the Čerenkov radiation is a result of the interference of the above BS shock waves.We quote them:

> "Summing up, one can say that radiation of a charge moving with the light velocity along the limited section of its path (the Tamm problem) is the result of interference of two bremsstrahlungs produced in the beginning and at the end of motion. This is especially clear when the charge moves in vacuum where the laws of electrodynamics prohibit radiation of a charge moving with a constant velocity. In the Tamm problem the constant-velocity charge motion over the distance l between the charge acceleration and stopping moments in the beginning and at the end of the path only affects the result of interference but does not cause the radiation.
>
> As was shown by Tamm [1] and it follows from our paper the radiation emitted by the charge moving at a constant velocity over the finite section of the trajectory l has the same characteristics in the limit $l \to \infty$ as the VCR in the Tamm-Frank theory [6]. Since the Tamm-Frank theory is a limiting case of the Tamm theory, one can consider the same conclusion is valid for it as well.
>
> Noteworthy is that already in 1939 Vavilov [10] expressed his opinion that deceleration of the electrons is the most probable reason for the glow observed in Čerenkov's experiments".

(We left the numeration of references in this citation the same as it was in Ref. [10]).
We agree with the authors of [10,11] that Tamm's approximate formulae (2.2) and (2.3) can be interpreted as the interference between two BS waves. This is due to the fact that Tamm's formulae do not describe the Čerenkov radiation properly. On the other hand, exact formulae found in [12] contain both the Čerenkov radiation and bremsstrahlung and cannot be reduced to the interference of two BS waves.
Further, we insist that Eq.(1.2) defining the field strength maxima in the Fourier representation is valid when the point charge moves with the velocity $v > c_n$ on the finite space interval small compared with the sphere radius R_0 ($z_0 << R_0$). When the value of z_0 is compared or larger than R_0, the pronounced maximum of the Fourier transforms of the field strengths at the angle $\cos\theta = 1/\beta_n$ disappears. Instead, many maxima of the same amplitude distributed over the finite region of space arise. In particular, for the infinite charge motion the above mentioned Fourier transforms are highly oscillating functions of space variables distributed over the whole space. Thus, Eq. (1.2) cannot be used for the identification of the Čerenkov radiation on large motion intervals.
However, in the usual space-time representation field strengths in the absence of dispersion have a singularity at the angle $\cos\theta = 1/\beta_n$. When the dispersion is taken into account, many maxima in the angular distribution of field strengths (in the usual space-time representation) appear, but the main maximum is at the same position where Čerenkov singularity lies in the absence of dispersion ([8]).

It should be noted that doubts on the validity of Tamm's formula (1.2) for the maximum of Fourier components were earlier pointed out by D.V. Skobeltzyne [19] on the grounds entirely different from ours. We mean the so-called Abragam-Minkowski controversy between photon energy and its momentum.

7 Appendix

We start from the Green function expansion in the cylindrical coordinates

$$G_\omega(\vec{r},\vec{r}') = -\frac{1}{4\pi}\frac{\exp(-ik_n|\vec{r}-\vec{r}'|}{|\vec{r}-\vec{r}'|} =$$

$$-\sum_{m=0}^{\infty}\epsilon_m\cos m(\phi-\phi')\{\frac{1}{4\pi i}\int_{-k_n}^{k_n}dk_z\exp[k_z(z-z')]G_m{}^{(1)}(\rho,\rho')+$$

$$+\frac{1}{2\pi^2}(\int_{-\infty}^{-k_n}+\int_{k_n}^{\infty})dk_z\exp[k_z(z-z')]G_m{}^{(2)}(\rho,\rho')\},$$

where

$$G_m{}^{(1)}(\rho_<,\rho_>) = J_m(\sqrt{k_n^2-k_z^2}\rho_<)H_m^{(2)}(\sqrt{k_n^2-k_z^2}\rho_>),$$

$$G_m{}^{(2)}(\rho_<,\rho_>) = I_m(\sqrt{k_z^2-k_n^2}\rho_<)K_m(\sqrt{k_z^2-k_n^2}\rho_>).$$

The Fourier component of VP satisfies the equation

$$(\Delta+k_n^2)A_\omega = -\frac{4\pi}{c}j_\omega, \qquad (A.1)$$

where $k_n = \omega/c_n > 0$ and $j_\omega = \delta(x)\delta(y)\exp(-i\omega z/v)/2\pi$ The solution of (A.1) is given by

$$A_\omega = \frac{1}{c}\int G_\omega(\vec{r},\vec{r}')j_\omega(\vec{r}')dV' =$$

$$= -i\pi\exp(-i\omega z/v)H_0^{(2)}(\frac{\omega\rho}{v}\sqrt{\beta_n^2-1})$$

for $\beta_n > 1$ and

$$= 2\exp(-i\omega z/v)K_0(\frac{\omega\rho}{v}\sqrt{1-\beta_n^2})$$

for $\beta_n < 1$. Separating the real and imaginary parts, we arrive at (5.5). Equating (5.4) and (5.5) and collecting terms at $\sin(\omega z/v)$ and $\cos(\omega z/v)$, we get the integrals

$$\int_0^\infty \cos(\frac{\omega\rho}{v}\sinh\chi)\sin(\frac{\omega\rho}{c_n}\cosh\chi)d\chi =$$

$$= \int_0^\infty \cos(\frac{\omega\rho}{v}x)\sin(\frac{\omega\rho}{c_n}\sqrt{x^2+1})\frac{dx}{\sqrt{x^2+1}} = \int_1^\infty \cos(\frac{\omega\rho}{v}\sqrt{x^2-1})\sin(\frac{\omega\rho}{c_n}x)\frac{dx}{\sqrt{x^2-1}} =$$

$$= \frac{\pi}{2}J_0(\frac{\omega\rho}{v}\sqrt{\beta_n^2-1})$$

for $v > c_n$ and $= 0$ for $v < c_n$.

$$\int_0^\infty \cos(\frac{\omega\rho}{v}\sinh\chi)\cos(\frac{\omega\rho}{c_n}\cosh\chi)d\chi =$$

$$= \int_0^\infty \cos(\frac{\omega\rho}{v}x)\cos(\frac{\omega\rho}{c_n}\sqrt{x^2+1})\frac{dx}{\sqrt{x^2+1}} = \int_1^\infty \cos(\frac{\omega\rho}{v}\sqrt{x^2-1})\cos(\frac{\omega\rho}{c_n}x)\frac{dx}{\sqrt{x^2-1}} =$$

$$= -\frac{\pi}{2}N_0(\frac{\omega\rho}{v}\sqrt{\beta_n^2-1})$$

for $v > c_n$ and $= K_0(\frac{\omega\rho}{v}\sqrt{1-\beta_n^2})$ for $v < c_n$. As we have mentioned, we did not find these integrals in the available mathematical literature.

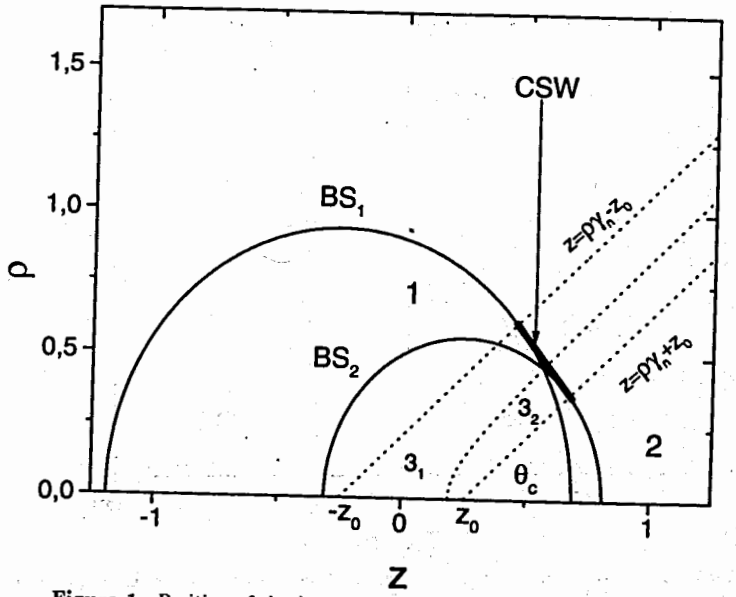

Figure 1. Position of shock waves at the fixed moment of time. BS_1 and BS_2 are bremsstrahlung shock waves emitted at the points $\mp z_0$ of the z axis. The solid segment between the lines $z = \rho\gamma_n - z_0$ and $z = \rho\gamma_n + z_0$ is the Čerenkov shock wave (CSW).

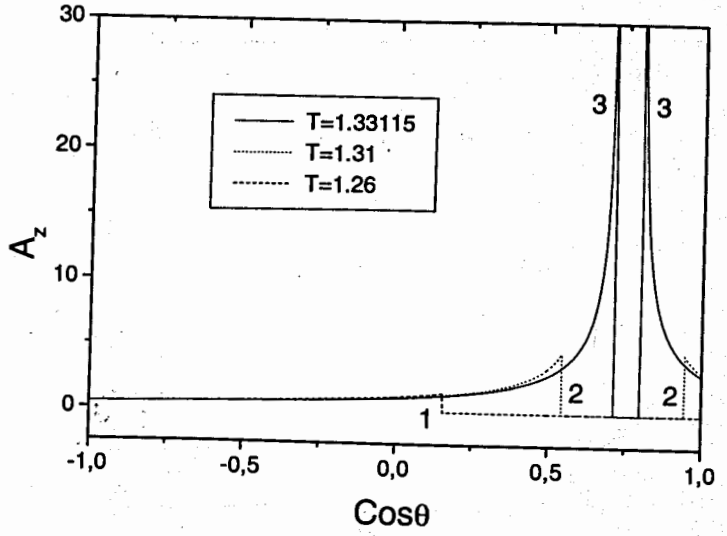

Figure 2. Time evolution of shock waves on the surface of the sphere S_0. For small times the BS shock wave occupies only back part of S_0 (curve 1). For larger times the BS shock wave begin to fill the front part of S_0 as well (curve 2). The jumps of BS shock waves are finite. The jump becomes infinite when the BS shock wave meets CSW (curve 3). A_z is in units e/R_0, time $T = ct/R_0$

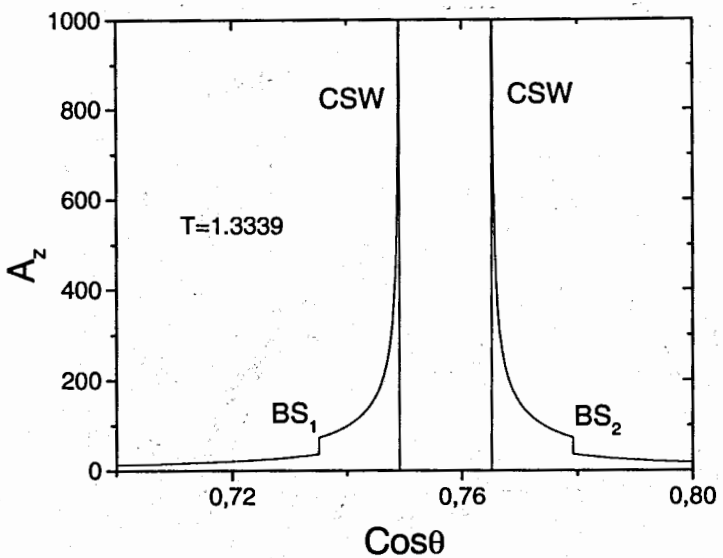

Figure 3. Further time evolution of shock waves on the surface of the sphere S_0. The amplitude of Čerenkov's shock wave is infinite while BS shock waves exhibit finite jumps.

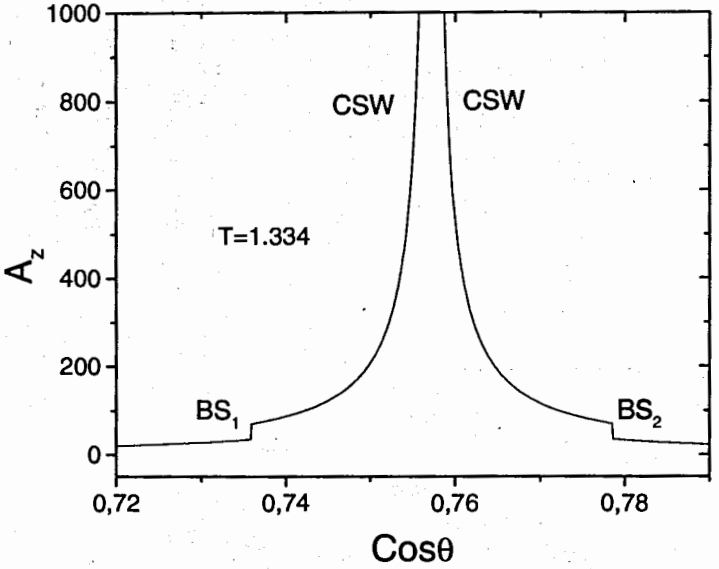

Figure 4. Position of CSW and BS shock waves at the moment when CSW touches the sphere S_0 only at one point.

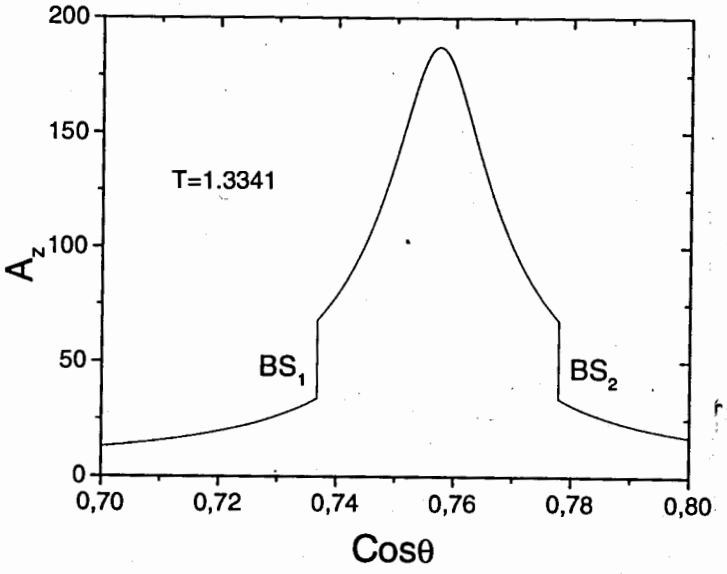

Figure 5. The Čerenkov post-action and BS shock waves after the moment when CSW has left S_0.

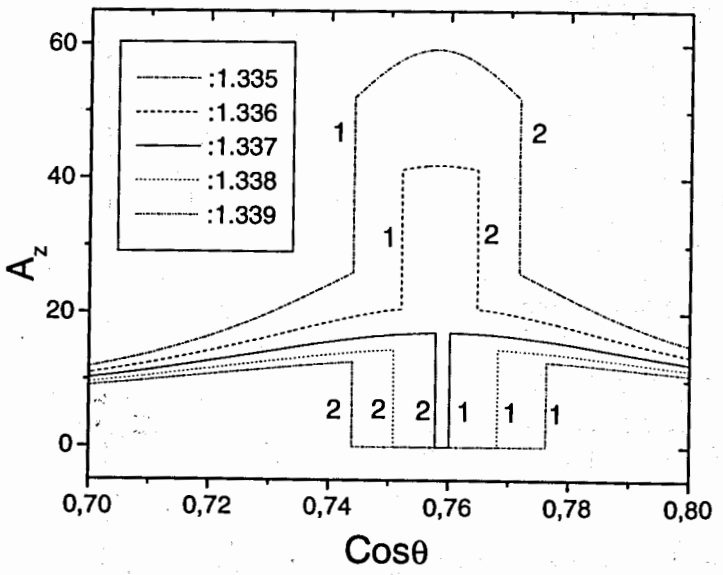

Figure 6. Further time evolution of BS shock waves on the surface of the sphere S_0. They approach and pass through each other leaving after themselves the zero electromagnetic field. Numbers 1 and 2 mean BS_1 and BS_2 shock waves, resp.

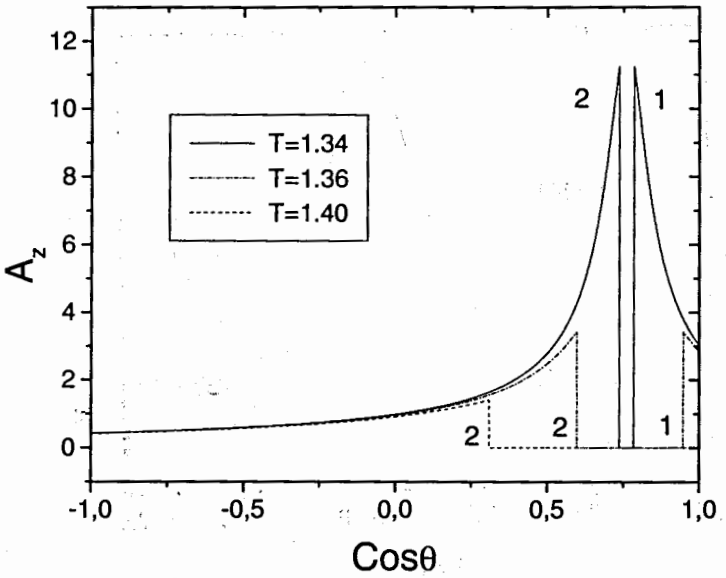

Figure 7. Further time evolution of BS shock waves on the surface of the sphere S_0. After some moment BS shock wave begin to fill only the back part of S_0. Numbers 1 and 2 mean BS_1 and BS_2 shock waves, resp.

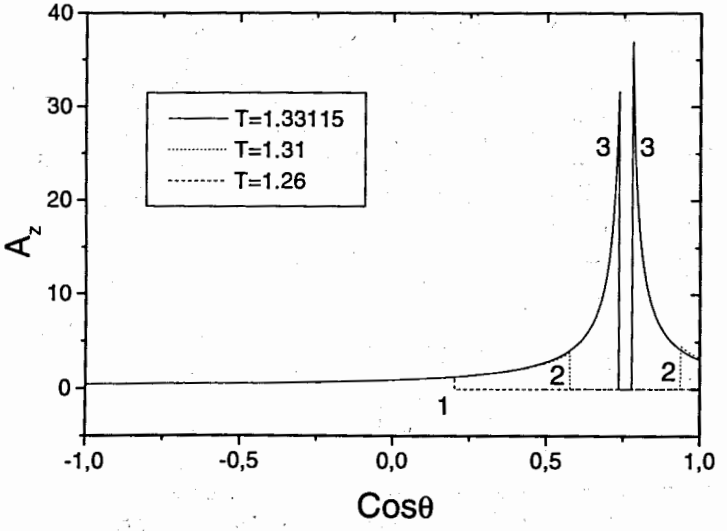

Figure 8. Time evolution of BS shock waves according to Tamm's approximate picture. The jumps of BS shock waves are finite. After some moment BS shock waves fill both the back and front parts of S_0 (curves 2 and 3).

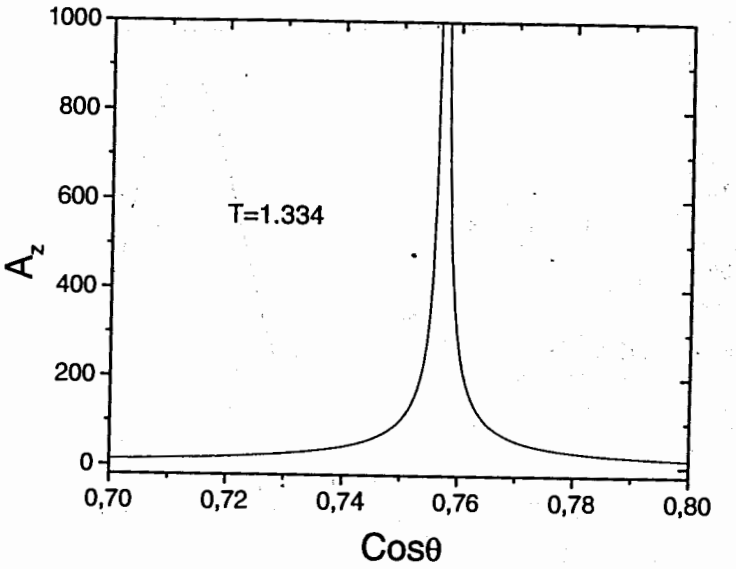

Figure 9. Position of the BS shock wave in Tamm's approximate picture at the moment when its jump is infinite.

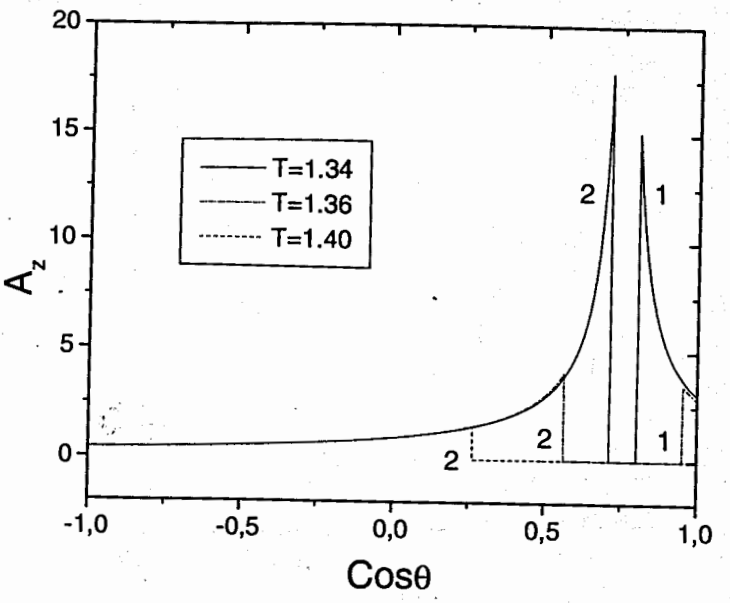

Figure 10. Further time evolution of BS shock waves in Tamm's approximate picture on the surface of the sphere S_0. After some moment BS shock waves fill only the back part of S_0. Numbers 1 and 2 mean BS_1 and BS_2 shock waves, resp.

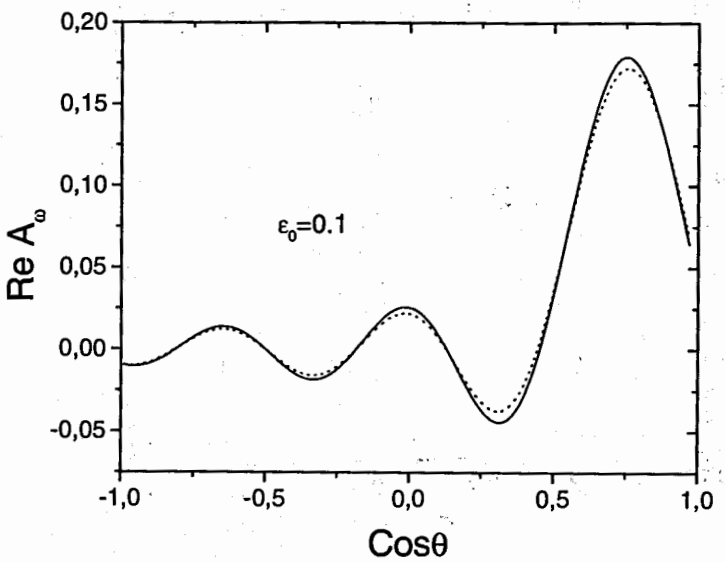

Figure 11. The real part of the VP Fourier transform (in units $e/2\pi c$) on the surface of S_0 for $\epsilon_0 = z_0/R_0 = 0.1$. The radiation field differs essentially from zero in the neighborhood of the Čerenkov critical angle $\cos\theta_c = 1/\beta_n$. The solid and dotted curves refer to the exact and approximate formulae (2.1) and (2.2), resp. It turns out that a small difference of the Fourier transforms is responsible for the appearance of the Čerenkov radiation in the space-time representation.

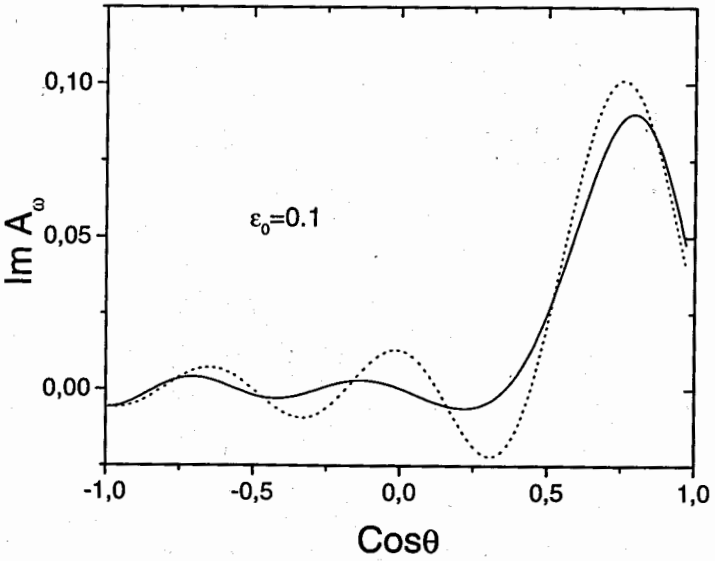

Figure 12. The same as in Fig. 11, but for the imaginary part of VP.

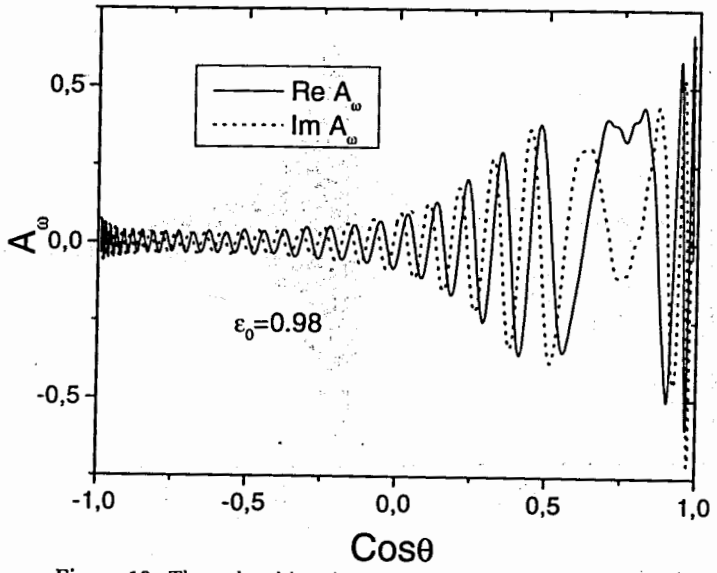

Figure 13. The real and imaginary parts of A_ω for $\epsilon_0 = 0.98$. The electromagnetic radiation is distributed over the whole sphere S_0.

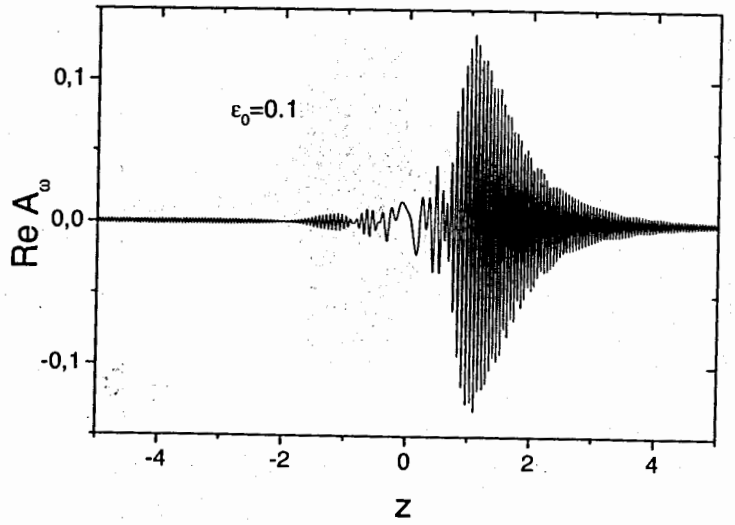

Figure 14. The real part of A_ω on the cylinder C surface for the ratio of the interval motion to the cylinder radius $\epsilon_0 = 0.1$. The electromagnetic radiation differs from zero in the neighborhood of $z = \gamma_n$, that corresponds to $\cos\theta_c = 1/\beta_n$ on the sphere (z is in units ρ, A_ω in units $e/2\pi c$).

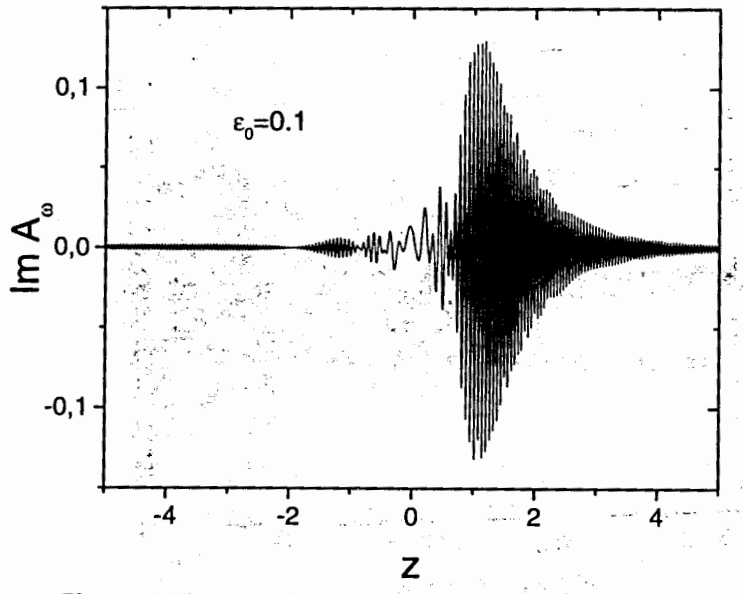

Figure 15. The same as in Fig. 14, but for the imaginary part of A_ω.

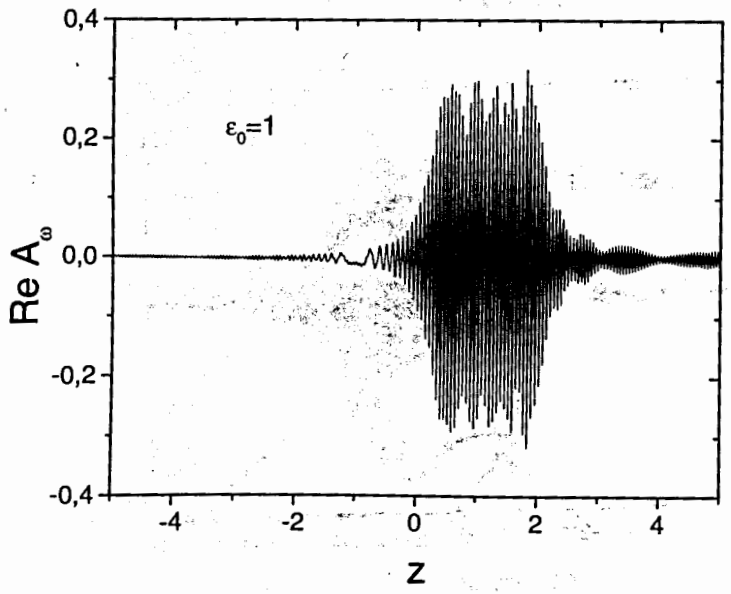

Figure 16. The same as in Fig. 14, but for $\epsilon_0 = 1$. There is no sharp radiation maximum at the neighborhood of $z = \gamma_n$.

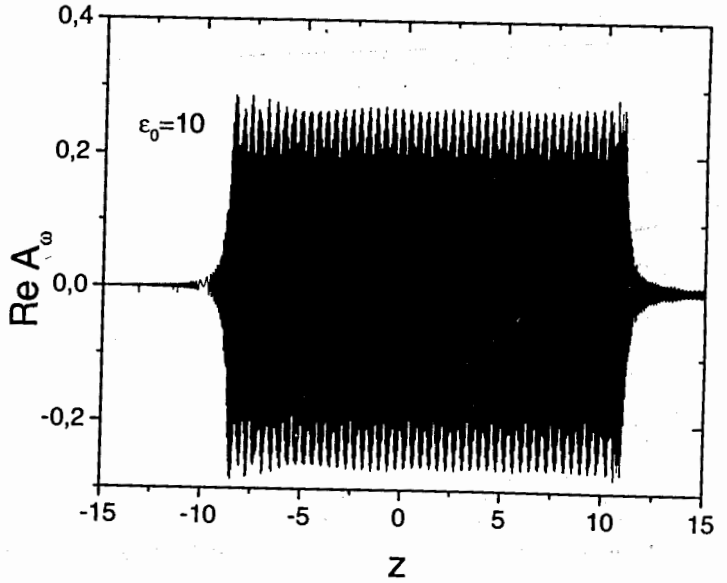

Figure 17. The same as in Fig. 14, but for $\epsilon_0 = 10$. There is no radiation maximum at the neighborhood of $z = \gamma_n$ and the radiation is distributed over the large z interval.

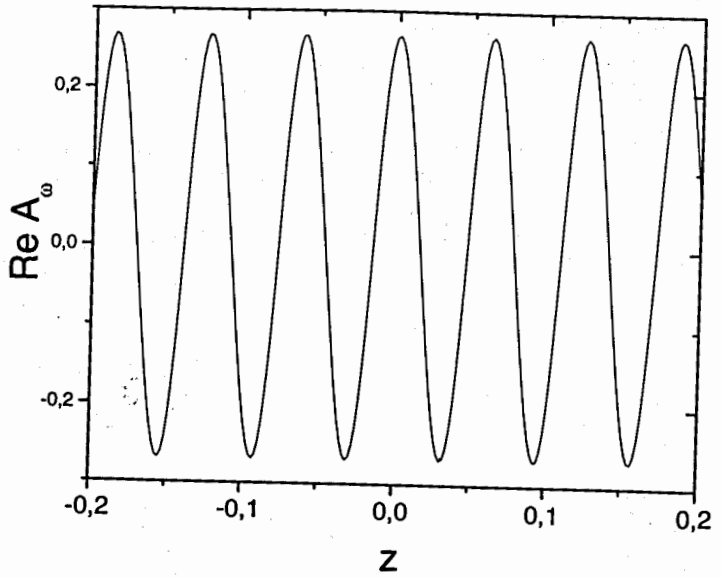

Figure 18. The same as in Fig. 17, but for small z interval. On this interval $Re A_\omega$ evaluated according to Eq.(5.4) for $\epsilon_0 = 10$ and according to Eq.(5.5) for the infinite motion interval are indistinguishable.

8 References

1. O. Heaviside, 1888, Electrician (Nov. 23), 83; 1889, Phil. Mag., 27, 324; 1912, *Electromagnetic Theory*, vol. 3 (London, The Electrician).
2. P.A. Čerenkov, 1934, Dokl. Acad. Nauk USSR, 2, 451.
3. A.A. Tyapkin, 1974, Usp. Fiz. Nauk, 112, 731.
4. T.R. Kaiser, 1974, Nature, 274, 400.
5. I.M. Frank and I.E.Tamm, 1937, Dokl. Acad. Sci. USSR, 14, 107.
6. Tamm I.E., 1939, J. Phys. USSR, 1, No 5-6, 439-461.
7. Frank I.M., 1988, *Vavilov-Čerenkov Radiation. Theoretical Aspects* (288 pages) (Moscow: Nauka).
8. Afanasiev G.N. and Kartavenko V.G., 1998, J.Phys. D: Applied Physics, v. 31, No 20, 2760-2776;
Afanasiev G.N., Kartavenko V.G. and Magar E.N., 1998, *Vavilov-Čerenkov radiation in dispersive medium* , JINR Preprint E2-98-98 (to appear in 'Physica B').
9. Landau L.D. and Lifshitz E.M., 1992, *Electrodynamics of Continuous Media*, (Oxford:Pergamon).
10. Zrelov V.P. and Ruzicka J., 1989, Chech.J.Phys. B, 368-383.
11. Zrelov V.P. and Ruzicka J., 1992, Chech.J.Phys., 42, 45-57.
12. Afanasiev G.N., Beshtoev Kh. and Stepanovsky Yu.P., 1996, Helv. Phys. Acta, 69, 111-129.
13. Kobzev A.P. and Frank I.M., 1981, Yadernaya Fizika, 334, 134-137.
14. Ginzburg V.L. and Tsytovich V.N., 1984, *Transition radiation and transition scattering*(Moscow, Nauka), in Russian.
15. Bowler M.G., 1996, Nucl. Instr. and Methods in Phys. Res. A, 378, 463-467.
16. Ginzburg V.L., 1940, Zh.Eksp.Teor.Fiz., 10, 589; 1940, J.Phys. USSR, 3, 101.
17. Akhiezer A.I. and Berestetzky V.B., 1981, *Quantum Electrodynamics* (Moscow: Nauka).
18. Glauber R., 1965, in *Quantum Optics and Electronics* (Lectures delivered at Les Houches, 1964, Eds.: C.DeWitt, A.Blandin and C.Cohen-Tannoudji), p.93-279,(New York: Gordon and Breach).
19. Skobeltzyne D.V., 1975, C.R. Acad. Sci.Paris, Ser.B, 280, 251-254; 287-290; 1977, Usp. Fiz. Nauk, 122, No 2, 295-324.

Received by Publishing Department
on January 18, 1999.